



Understanding the inter-city causality and regional transport of atmospheric PM_{2.5} pollution in winter in the Harbin-Changchun megalopolis in China: A perspective from local and regional

Bo Li ^{a,b}, Xiaofei Shi ^{a,b,d}, Jinpan Jiang ^{a,b}, Lu Lu ^a, Li-xin Ma ^{a,b}, Wei Zhang ^c, Kun Wang ^{a,b}, Hong Qi ^{a,b,*}

^a School of Environment, Harbin Institute of Technology, Harbin, 150090, China

^b State Key Laboratory of Urban Water Resource and Environment, Harbin Institute of Technology, Harbin, 150090, China

^c School of Computer Science and Technology, Harbin Institute of Technology, Harbin, 150090, China

^d CASIC Intelligence Industry Development Co., Ltd, Beijing, 100854, China

ARTICLE INFO

Handling editor: Aijie Wang

Keywords:

Cold urban agglomeration
PM_{2.5} pollution
Convergent cross mapping
CMAQ-BFM
Inter-city causality
Regional transport

ABSTRACT

Harbin-Changchun megalopolis (HCM) is the typical cold urban agglomeration in China, where PM_{2.5} pollution is still serious in winter against the backdrop of continuous improvement in annual air quality in China. To further understand interactions of atmospheric pollution among HCM cities, inter-city causality and regional transport of PM_{2.5} in the winter in the HCM were comprehensively investigated by using convergent cross mapping (CCM) and CMAQ-BFM methods. CCM analysis results suggest strong bidirectional causal relationships between cities in the HCM, and the causality during polluted episodes were significantly larger than that during clean period. In addition, the influence on local PM_{2.5} from the HCM western cities were larger than that from cities in the southeast. Inter-city and regional transport contributions results demonstrated that although local emission were the largest contributors among 14 sub-regions for most HCM cities, interactions among cities were strong. Regional transport (42.8%–77.4%) largely contributes to HCM cities' PM_{2.5} concentrations. Among three regions outside the HCM, NMG (including part of inner Mongolia and Baicheng city in Jilin, 9.1%) was the largest contributor to the PM_{2.5} concentration in the whole HCM, followed by JLS (including Liaoning Province, Tonghua and Baishan cities in Jilin province, 5.1%) and HLJ (including cities of Heihe, Yichun, Jiamusi, Hegang, Shuangyashan, Jixi, Qitaihe in the Heilongjiang province, 3.8%). Regional transport contribution to the most HCM cities increased significantly from excellent to heavily polluted days. Furthermore, close relationships between transport paths/intensity and wind direction/speed in studied region suggests that we can quantitatively guide the regional joint emergency prevention and control before and during heavily polluted events based on regional weather forecasts in the future.

1. Introduction

In recent years, rapid economic development, industrialization and urbanization process have led to a significant increase in anthropogenic air pollutant emissions in China (Huang et al., 2018). Haze pollution has attracted great attention in China during the past years (Li et al., 2020) due to its adverse impact on human health (Chang et al., 2019; Sun et al., 2020), atmospheric visibility, regional air quality, and climate change (Wang et al., 2019a; Yang et al., 2020a). Haze is the impairment of visibility caused by the small particular, especially PM_{2.5}, scattering and

absorbing light in the atmosphere (Boylan and Russell, 2006). The annual average concentration of PM_{2.5} in major metropolitan areas in China have decreased over the years because of the strict control measures taken by the Chinese government (Wang et al., 2019a). However, it should be noted that severe haze still occurs in winters in many major regions, especially in the cold urban agglomeration in China.

Harbin-Changchun megalopolis (HCM) is the typical cold urban agglomeration in China, which is a mainly industrial and grain production base of China (Chen et al., 2017; Li et al., 2020). HCM is located in the central northeast of China (112°30' - 116°10' E and 29°05' -

* Corresponding author. State Key Laboratory of Urban Water Resource and Environment, Harbin Institute of Technology, 73 Huanghe Road, Nangang District, Harbin, Heilongjiang, 150090, China.

E-mail address: hongqi@hit.edu.cn (H. Qi).

31°50' N) including 11 prefecture-level cities: Qiqihar (QQHR), Daqing (DQ), Changchun (CC), Harbin (HRB), Sanyuan (SY), Siping (SP), Liaoyuan (LY), Jilin (JL), Suihua (SH), Mudanjiang (MDJ), and Yanbian Korean Autonomous Prefecture (YB). The regional area of HCM is about 263,640 km², and the population density is 149.8 per km². The HCM is affected by high-latitude monsoon climate with a cold and dry winter (Guo et al., 2019). Although the annual average PM_{2.5} concentration in the HCM decreased 32.0% (approximately 16.1 µg/m³) from 2015 to 2020, but from a seasonal perspective the average PM_{2.5} concentration was not always decreasing. The average PM_{2.5} concentration in the winter sharply decreased by 24.6% (approximately 23.1 µg/m³) from 2015 to 2016 and fluctuated slightly ($61.9 \pm 7.7 \mu\text{g}/\text{m}^3$) from 2016 to 2020 (coefficient of variation less than 0.15). These results demonstrate that PM_{2.5} pollution is still serious in winter in the HCM. Therefore, it is necessary to further understand the interaction between the HCM cities, which could provide useful information for the air quality improving in winter in typical cold region. To the best of our knowledge, causality analysis can prove the underlying interaction of PM_{2.5} pollution among HCM cities, but the interaction mechanism of PM_{2.5} pollution is unclear. Inter-city and regional transport of atmospheric pollutants may have great contributions to the haze pollution formation in winter in the HCM (Dong et al., 2020; Qiao et al., 2019a). For example, according to the works by Dong et al. (2020) (Dong et al., 2020) and Wang et al. (2015) (Wang et al., 2015), the regional transport contributions to PM_{2.5} were even larger than 50% in some cities in Hebei province, China. Hence, it is essential to quantify the inter-city causality and regional transport of atmospheric PM_{2.5}, which is of great significance for developing effective control strategies to improve the air quality in the HCM. Thus, as an important part of determining the causal relationship of PM_{2.5} pollution among cities, inter-city and regional transport contributions were usually investigated to quantitatively clarify the interaction mechanism between local and regional PM_{2.5} pollution.

Previous researches mostly focus on the spatiotemporal distribution characteristics of air pollutants in a certain city and/or small region in the HCM (Chen et al., 2017; Li et al., 2020), while researches exploring the interaction among cities within large region is scarce. Convergent cross mapping (CCM) method posed by Sugihara et al. (2012) (Sugihara et al., 2012) has been proved to be useful in extracting the causality between two time series datasets from complex atmospheric system (Chen et al., 2016; Sugihara et al., 2012), which resolves the problem that correlation does not imply causation. In addition, chemical transport model (CTM) with sensitivity analysis methods are effective approaches for the quantitative research on regional transport contributions, which can determine the source of particulate matter from a specific region to the target region at the local, regional, and intercontinental scale (Qu et al., 2021). There are three sensitivity analysis methods including the brute force method (BFM) (Huang et al., 2018; Qiao et al., 2019a), decoupled direct method (DDM) (Bates et al., 2018; Chatani et al., 2020), and tracer-based approaches (Chang et al., 2019; Dong et al., 2020; Li et al., 2019), which are often used to quantify the transport contributions. Li et al. (2019) used a regional air quality model (RAMS-CMAQ-ISAM) to study the transport contributions of PM_{2.5} in typical Chinese regions (Li et al., 2019). The result demonstrated that the regional contributions to PM_{2.5} in most provinces have large variations and the local emission contributions vary from approximately 25%–40%. Wu et al. (2013) reported that the regional contribution of PM_{2.5} from the surrounding region to Guangzhou in December 2011 reached up to 70% by using the model of CAMx-PAST (Wu et al., 2013). Huang et al. (2018) used the CMAQ model with the BFM to investigate the local and remote region transport contribution to the fine particulate matter in Guangzhou and Foshan (Huang et al., 2018). The result showed that the regional contribution from the surrounding area to Guangzhou and Foshan were 46–61% and 57.8–72.9%, respectively. In the Beijing-Tianjin-Hebei (BTH), research suggests that regional transport contribution to total fine particulate matter by 2.5%–68.4% in 2017 (Dong et al., 2020). Hence, there is a large variation in

regional transport contributions to PM_{2.5} concentration in different regions and seasons. However, the researches on regional transport contribution to PM_{2.5} are concentrated in several economically developed regions including BTH (Dong et al., 2020; Wang et al., 2019b), Yangtze River Delta (YRD) (Fu et al., 2016; Li et al., 2015), Pearl River Delta (PRD) (Huang et al., 2018; Qu et al., 2021), and Chengyu area (Qiao et al., 2019a, 2019b) in China, and few study attempts to explore inter-city and regional transport of atmospheric PM_{2.5} in the HCM. Therefore, the roles of regional transport in haze formation during winter in the HCM needs to be further clarified.

December and January are the most heavily polluted winter-time, and 2017 were a peak year of annual average PM_{2.5} concentration in the HCM in recent years. Therefore, period from December 22, 2016 to January 22, 2017 including several clean and polluted episodes were selected in this study to (1) explore the causal relationships between local and regional atmospheric PM_{2.5} pollution by using CCM method; (2) quantify the transport contributions to PM_{2.5} concentrations among the cities in the HCM and the surrounding regions; (3) identify the transport paths of PM_{2.5} during different haze episodes. Overall, current research systematically explores the inter-city causality and regional transport of atmospheric PM_{2.5} pollution from local and regional perspective, in which case researchers can better understand the interaction among cities within the HCM. Furthermore, results derived from current study could provide useful information not only long-term emission control strategy, but also the emergency control actions before and during a heavy pollution episode.

2. Data source, statistical methods, and model setup

Hourly real-time air pollutants and meteorological data at monitoring sites in the HCM (Fig. 1(b)) from December 22, 2016 to January 22, 2017 were utilized for the model evaluations. The geographical location information of these monitoring sites was shown in support information file (Table S1 and Table S2). The National Centre for Environmental Prediction FNL (Final) operational global analysis datasets were obtained as the initial meteorological and boundary condition of the weather research and forecasting (WRF) model (NCEP, 1999). The monthly Multi-resolution Emission Inventory for China inventory (MEICv1.3, <http://www.meicmodel.org/>) (Li et al., 2017; Zheng et al., 2018) for the base year of 2016 and 2017 developed by Tsinghua University with a spatial resolution of 0.25° by 0.25° were used as inputs for CMAQ model. WRFv3.9.1 model was applied to simulate the meteorological fields and meteorological driver for SMOKEv4.0 and CMAQv5.2 model. Two nested domains were used in this study, and the inner domain with a spatial resolution of 12 km covered the HCM regions and several surrounding cities, as shown in Fig. 1. To better understand the transport contributions and pathways of air pollutants in the study area, the inner domain was divided into 14 subdomains according to the pollutant emission and geographical location, as shown in Fig. 1(b). From number 1 to number 14, the cities and regions are QQHR, SH, DQ, SY, HRB, CC, SP, LY, JL, YB, MDJ, NMG including part of inner Mongolia and Baicheng city in Jilin, HLJ including 7 cities in the northeast Heilongjiang (Heihe, Yichun, Jiamusi, Hegang, Shuangyashan, Jixi, Qitaihe), JLS including Liaoning Province, Tonghua and Baishan cities in Jilin province.

Moreover, considering the BFM as a suitable approach to simulate the non-linear relationship between particulate matter and its precursors under large emission changes (Wang et al., 2015), CMAQ with BFM was used to investigate the local and regional transport contributions of particulate matter in the HCM region. Briefly, Carbon Bond 05 gaseous chemical scheme (CB05) (Yarwood, 2005) and the Aero 6 aerosol scheme (AERO6) (Appel et al., 2017) were used for CMAQ model. In addition, as the study period of this study was from December 22, 2016 to January 24, 2017 and December 11th - December 21st, 2016 was set up as spin-up days in order to minimize the impact of initial conditions on the simulation results. In addition, hourly BFM results

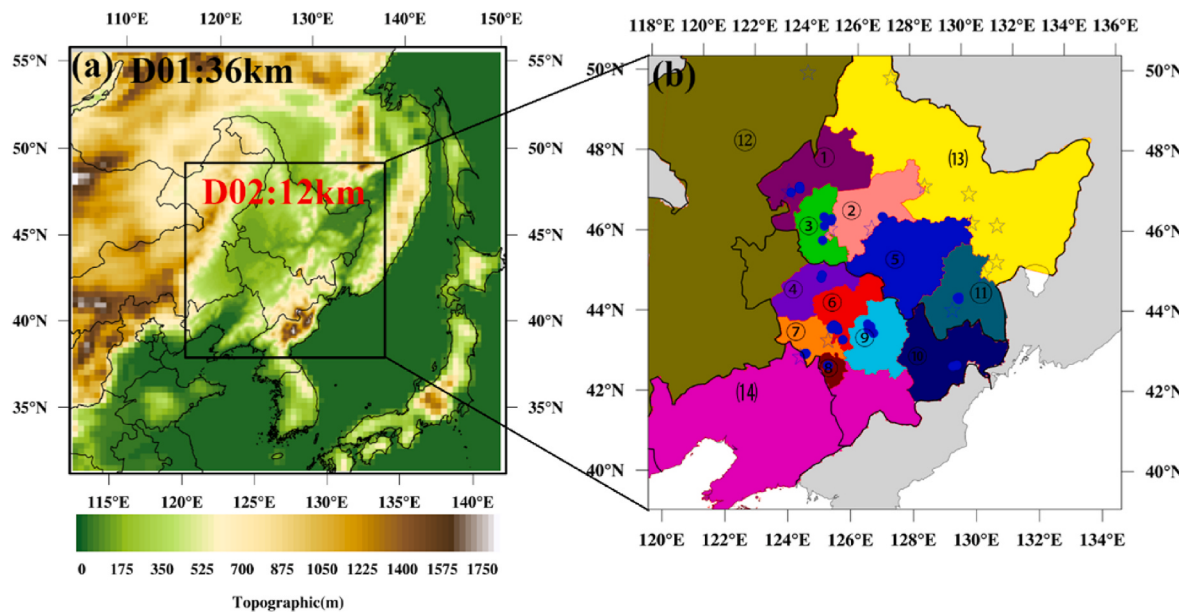


Fig. 1. (a) Topographic of two nested simulation domains (D01 and D02, 36–12 km resolution). (b) Locations of monitor sites for model evaluation in D02. Blue dots and blue stars are air pollutants and meteorological observation stations in HCM. Circled numbers mark Harbin-Changchun megalopolis (HCM) and its surrounding regions. From number 1 to number 14, the cities and regions are QQHR, SH, DQ, SY, HRB, CC, SP, LY, JL, YB, MDJ, NMG including part of inner Mongolia and Baicheng city in Jilin, HLJ including 7 cities in the northeast Heilongjiang (Heihe, Yichun, Jiamusi, Hegang, Shuangyashan, Jixi, Qitaihe), JLS including Liaoning Province, Tonghua and Baishan cities in Jilin province.

were employed to conduct the source sensitivity simulation for investigating the local and transport contribution to air pollutants by performing a number sensitivity experiments, of which one sub-region emission source was switched off (Burr and Zhang, 2011). Then, the different between sensitive experiments and baseline experiments were calculated to cross-regional source contributions (Huang et al., 2018). More detailed model configuration of WRF-CMAQ could be found in the Text S2 and Table S3. In addition, the grided hourly model-ready emission fields for CMAQ model was conducted by using the Sparse Matrix Operator Kernel Emissions (SMOKE) model. More detailed of emission inventory allocation processes were presented in the support information file (Text S2 and Table S4 - Table S6).

In general, CCM method combined with Pearson correlation analysis were conducted to investigate the interactions of PM_{2.5} concentrations among cities in the HCM. CCM method was conducted to quantitatively analysis the bidirectional causality between local and regional PM_{2.5} concentrations with few minor modifications (Chen et al., 2016; Li et al., 2020). Briefly, two time-series variables of the city hourly average concentrations of PM_{2.5} ($\mu\text{g}/\text{m}^3$) in the HCM region during the January were used for causality and correlation analysis. The city hourly average surface PM_{2.5} concentration datasets were collected from publishing website of China National Environmental Monitoring Centre (CNEMC, <http://113.108.142.147:20035/emcpublish/>). The key parameters of number of dimensions for the attractor reconstruction (E) and time lag (τ) used in the CCM method were set to 3 and 2 h, respectively (Li et al., 2020). The causality was determined according to the convergence map. The strength of influence from one dataset on another one was presented via the value of predictive skills (ρ) with the range from 0 to 1. If curve in the convergence map presented a convergence near the predictive skills values with the time series length increasing, then the causality between two cities' PM_{2.5} pollution was extracted, else there was no causality existence between these two cities' PM_{2.5} pollution. The CCM algorithms was built by using the Python program in this study. More detailed information of CCM method can be found in previous studies (Chen et al., 2016; Li et al., 2020).

3. Results and discussion

3.1. Model evaluations

In this study, the hourly observation data from 13 meteorological monitoring sites (Fig. 1(b)) were used to evaluate the performance of the WRF model by comparing it with the simulation results. In general, the performance of WRF in this study was comparable to previous studies (Huang et al., 2021; Wu et al., 2013; Yang et al., 2020b; Zhang et al., 2014) and the simulation results of WRF is acceptable, which can be used to drive the CMAQ model. More detailed information of the performance of WRF model can be found in the Text S3 and Table S7. Moreover, hourly observation datasets of the six criteria air pollutants from the HCM including 56 monitoring sites were collected to investigate the performance of the CMAQ model. The time series of hourly simulated and monitored air pollutants mass concentration averaged from 56 national standard air quality observation sites is presented in Fig. 2. For the CMAQ model, several statistical parameters including mean bias (MB), normalized mean bias (NMB), correlation coefficient (R), index of agreement (IOA), and the fraction of predictions within a factor of two of observations (FAC2) were used to evaluate the model performance. In this study, the patterns of observations and simulations of particulate matter (PM_{2.5} and PM₁₀) were very similar to those reported in previous studies (Qu et al., 2021; Wang et al., 2017; Yang et al., 2020a, 2020b). The values of R and IOA for PM_{2.5} (PM₁₀) were 0.82 (0.77) and 0.88 (0.85), respectively. A significant positive correlation between observation and simulation demonstrated that the model could well capture the temporal variations in PM concentrations. Lower NMB (< 15%) and higher FAC2 values (> 83%) of PM indicated a good performance of the CMAQ model in the simulation of PM, and this model was reliable to quantify the regional transport of PM_{2.5}. As shown in Fig. 2, among six criteria air pollutants, NO₂ has the lowest NMB (4%) and the highest IOA (0.87) and FAC2 (93%) values, which indicated a good agreement of the model simulation and observation results for NO₂. Furthermore, SO₂ and CO were underestimated by the model. This result was similar to the one reported in northeast China by Yang et al. (2020b) (Yang et al., 2020a), which can be attributed to the lack of

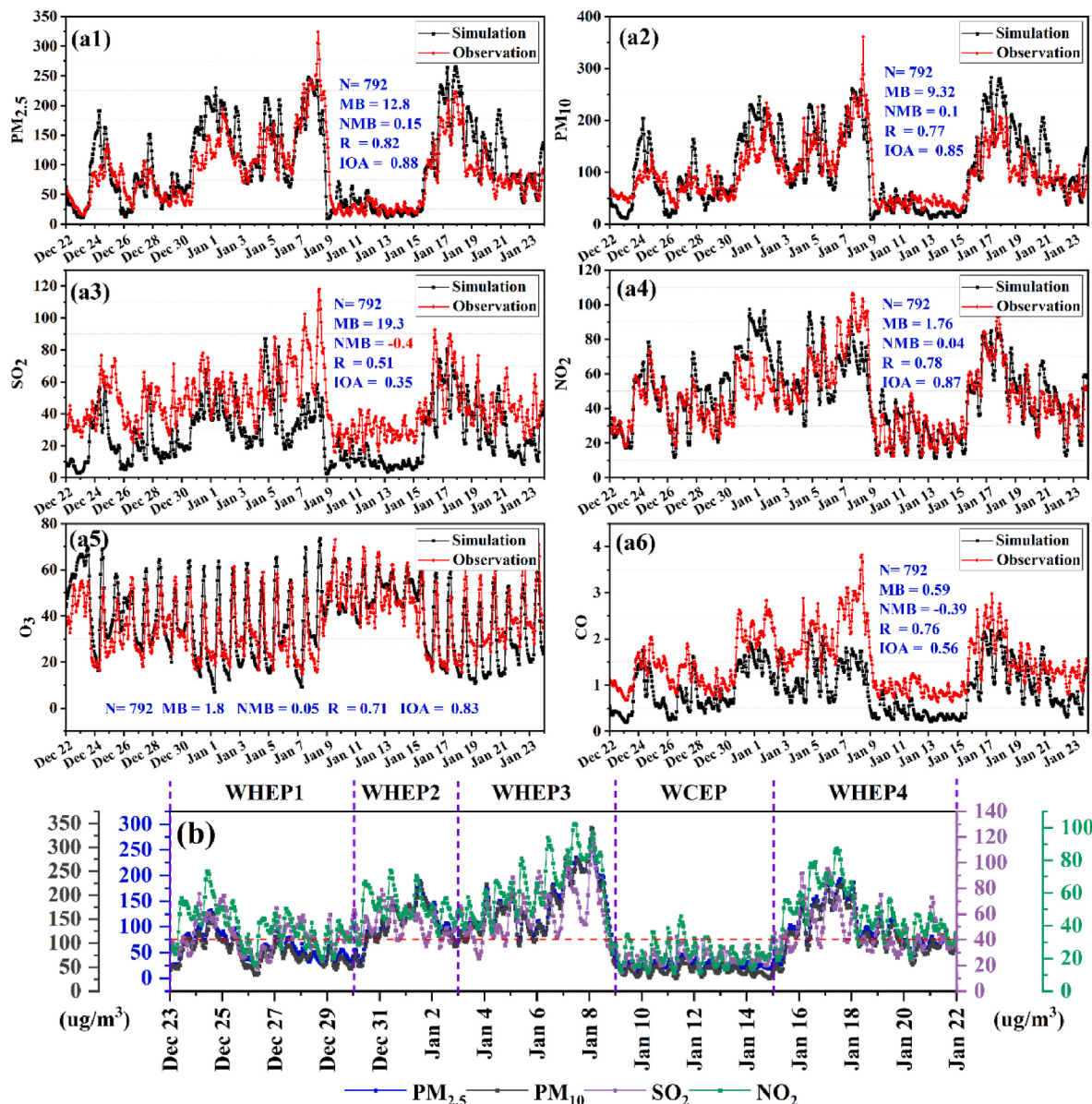


Fig. 2. (a) Comparing of the CMAQ simulated (black lines) and observational (red lines) concentrations of six air pollutants in the HCM, (b) Time series of air pollutants concentrations during different haze pollution episodes.

collected data on some potential anthropogenic emissions, such as household coal-fired heating (Zheng et al., 2018) and open biomass burning during winter (Yang et al., 2020a). However, the R values were 0.51 and 0.76 respectively, which indicated good agreement between observation and simulation results of SO₂ and CO.

3.2. Overview of pollution during the study period

Classification statistics of daily average concentration of PM_{2.5} and daily air quality index (AQI) in different HCM cities are presented in Table S8. According to AQI values, the days during the studied period can be divided into six classes: 0–50 (excellent), 51–100 (fine), 101–150 (slightly polluted), 151–200 (moderately polluted), 201–300 (heavy polluted), > 300 (serious polluted). Polluted days (AQI > 100) accounted for more than 40% of the studied period. The number of days with daily PM_{2.5} concentration exceeded 75 µg/m³ (the Chinese ambient air quality standards grade II for PM_{2.5}) during the studied period accounted for 61.8%, 44.1%, 50%, 52.9%, and 64.7% for HRB, DQ, CC, LY, and JL, respectively. These different pollution statuses among

different cities may be attributed to the different anthropogenic emission and particular topography and meteorological conditions of these cities, which played an important role in the accumulation, dispersion, and transformation of air pollutants (Li et al., 2018; Osada et al., 2009; Qiao et al., 2019a). Larger anthropogenic emissions of air pollutants and relatively lower topographic height (Fig. 1(b)) of HRB, SH, CC, SY, and JL cities resulted in the relatively higher mass concentration of air pollutants in these cities. According to the MEIC (Li et al., 2017; Zheng et al., 2018), the total emission of nine species including BC, CO, NH₃, NO_x, OC, PM_{2.5}, PM₁₀, SO₂, and VOCs from CC, HRB and SH accounted for approximately half (43.5%–48.8%) of the total emission from the whole HCM. Specifically, the annual emission of PM_{2.5}, SO₂, and NO_x from HRB are approximately 82,000 tons, 86,000 tons, and 213,000 tons, which account for 17.5%, 17.8%, and 18.2% of emissions in the HCM, respectively. For CC, the emission of PM_{2.5}, SO₂, and NO_x are 75,000, 87,500, and 204,000 tons per year accounting for 16%, 18%, and 17.5% of emission in the HCM. Moreover, according to statistics from the meteorological monitoring datasets, the days with the average wind speed below 3 m/s approximately accounted for 74% of the study

period.

To further understand the role of regional transport in the formation of PM_{2.5} pollution and identify the transport paths of PM_{2.5} during different pollution episodes, the whole studied period was divided into 4 p.m._{2.5} haze pollution episodes and one clean episode (Fig. 2(b)). The first three haze pollution episodes occurred during December 22nd - 29th, 2016 (WHEP1), December 30th, 2016–January 2nd, 2017 (WHEP2), and January 3rd - 8th, 2017 (WHEP3), which were controlled by low wind speed, and the dominant wind directions were westward (Fig. S1 (a-c)). Two of the most polluted cities during WHEP1 were JL

and SY with the peak PM_{2.5} concentrations of 156 and 176 µg/m³, respectively (Table S9). The most polluted city of WHEP2 and WHEP3 was Harbin with the mean PM_{2.5} concentrations of 182.3 (162–197) and 225.2 (145–296) µg/m³, respectively (Table S9). The clean episode (WCEP, January 9th - 14th, 2017) and the fourth haze pollution episode (WHEP4, January 15th - 22nd, 2017) were controlled by the northwest wind (Fig. S1 (d-e)). HRB and JL were still the two most polluted cities during WHEP4 and the mean concentrations of PM_{2.5} were 169.5 (89–270), and 154.7 (81–266) µg/m³, respectively (Table S9). According to Fig. S1 (b, e), there was an atmospheric wind vortex in HRB

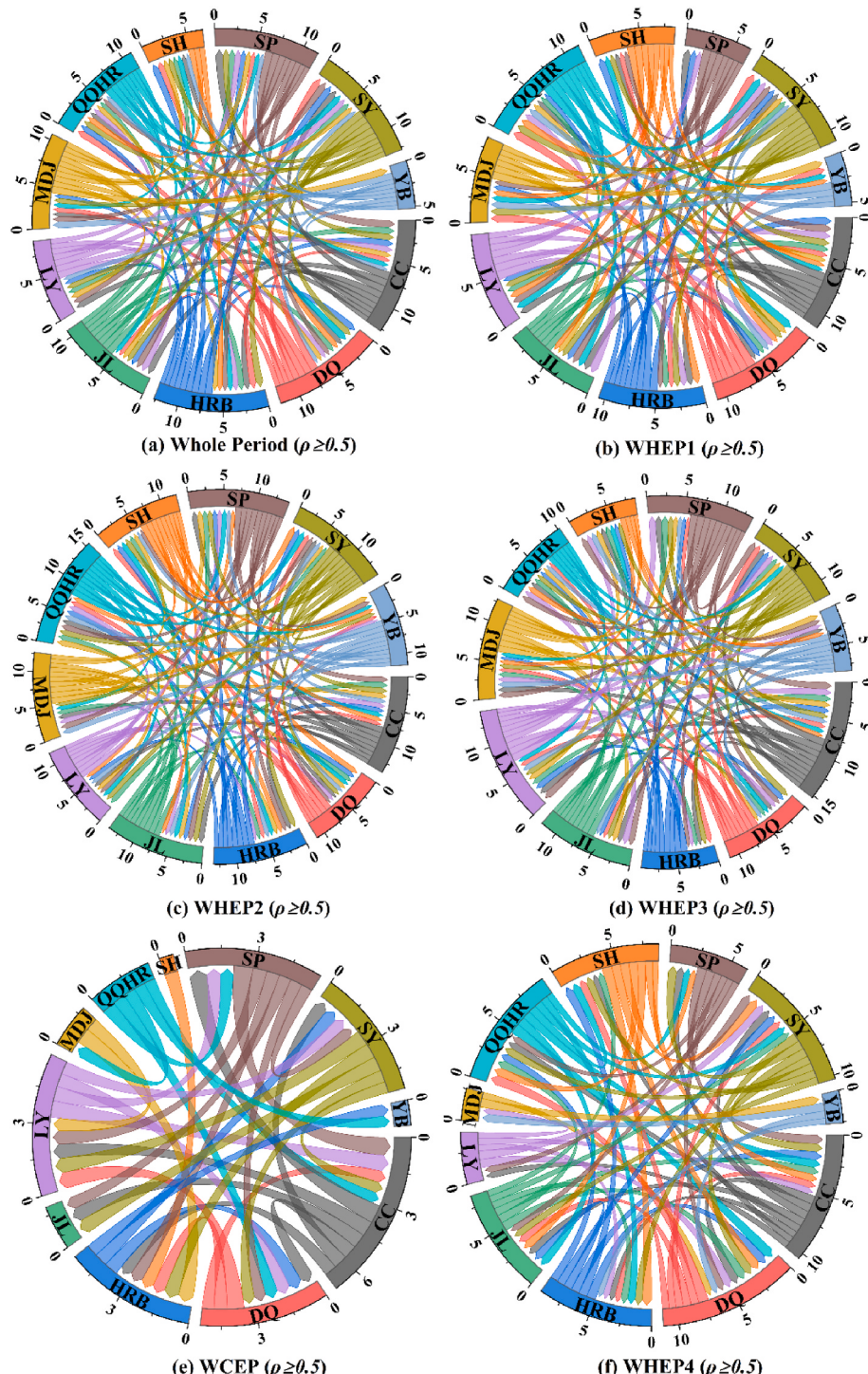


Fig. 3. The causality (ρ) of PM_{2.5} concentrations between cities within the HCM during different haze pollution episodes (Only the ρ greater or equal to 0.5 are presented in this figure and Arrow width and direction represents the magnitude and directions of the causal relationship, respectively).

and SH cities during WHEP2 and WHEP4, which might have resulted in the more moderately polluted (AQI >200) in Harbin (9 days, 26.5%) and SH (9 days, 26.5%) (Table S9).

3.3. The causal relationship among cities in the HCM

The causal relationships among cities during different pollution episodes in the HCM were investigated by using CCM method. The CCM results are shown in Fig. S2, and strong causal relationship ($\rho \geq 0.5$) between two cities were selected to presented in Fig. 3. CCM results demonstrates strong bidirectional causal relationships among cities in the HCM (Fig. 3(a)), and the average ρ value during the whole studied period was 0.6. This is to say, PM_{2.5} pollution in regional cities has a direct influence on the PM_{2.5} pollution in local city, and the local PM_{2.5} pollution also has significantly strong feedback influence on regional PM_{2.5} pollution. Moreover, it was obvious that local cities have larger influence on their neighboring cities than non-adjacent cities, and the influence on local PM_{2.5} pollution from cities in the west were larger than that from cities in the southeast. As shown in Fig. S3, the $\rho \geq 0.75$ were found mainly between adjacent cities. Take CC for instance, the average ρ value between CC and its' neighboring cities were 0.8 (to CC) and 0.8 (from CC), which was significantly larger than the average ρ value between CC and its' non-neighboring cities (to CC 0.52 and from CC 0.58). In addition, the first three strong causal relationship were to be found between CC and SP ($\rho = 0.91$), JL ($\rho = 0.82$) and SY ($\rho = 0.80$), and these cities were gathered in the west of CC, which were significantly larger than the causal relationship between CC with other cities ($\rho = 0.3-0.75$). This result may be attributed the regional geographical and meteorological conditions (Chen et al., 2016). Furthermore, atmospheric PM_{2.5} polluted level has significant influence on the causal relationship between cities within the HCM (Fig. 3(b-f)). The average ρ values during WHEP1, WHEP2, WHEP3, WCEP, and WHEP4 were 0.56, 0.70, 0.63, 0.31, and 0.51, respectively. In addition, the cities with ρ values more than 0.5 during WCEP significantly decreased compared to WHEP1-WHEP4. Obviously, the causality among cities within the HCM during polluted episodes (WHEP1-WHEP4) were significantly larger than that during clean period (WCEP). Moreover, the causal relationship during polluted episodes presented the following order: WHEP2 > WHEP3 > WHEP1 > WHEP4 (Fig. 3(b, c, d, f)). Stronger interactions between local and regional PM_{2.5} pollution in the HCM during polluted episodes suggests that it is necessary to implement a regional joint control strategy for the air quality improving in the HCM.

3.4. Inter-city and regional transport contributions to PM_{2.5} concentration in the HCM

3.4.1. Local contribution Vs. regional transport contribution

Although CCM results discussed above have demonstrated strong interactions between local and regional PM_{2.5} pollution, the mechanism on bidirectional causal relationships between regional and local city has not been explored. Therefore, inter-city and regional transport contributions were conducted to future quantitatively clarify the interaction between local and regional PM_{2.5} pollution in this study. The spatio-temporal variation of average inter-city and regional transport contributions to PM_{2.5} in the HCM cities are presented in Fig. 4. Transport contribution from "Others" can be attributed to initial and boundary conditions, and the nonlinearity in the PM_{2.5} formation reactions etc. (Huang et al., 2018; Qiao et al., 2019a). These parts contributed approximately 3.8% and 13.9% of the total PM_{2.5} concentrations in during the whole studied period in the HCM (Fig. 4(a)). In general, local emission contributions to PM_{2.5} in the HCM cities during the whole studied period were ranged from 12.4% to 48.5% with an average value of $25.9 \pm 10.7\%$. The largest contribution of local emission less than 50% demonstrated that regional transport was the dominant source for PM_{2.5} concentrations in cities within the HCM during the study period. Similar proportions between local source and regional transport

contribution also can be found in some typical Chinese regions during winter, where local emission contributions to PM_{2.5} in most provinces in China vary from approximately 25%–40% (Li et al., 2019). From the spatial perspective, largest local emission contribution was found in QQHR with the value of 48.5%, followed by SH (38.3%), CC (34.0%), and HRB (29.8%), which were significantly larger than that in other cities (12.1%–24.4%). Moreover, there are significant proportions variations of local source and regional transport contributions during different pollution episodes. As shown in Fig. 4 (b-f), local emission contributions during WHEP1, WHEP2, WHEP3, WCEP, WHEP4 were in ranges of 19.2%–48.3%, 10.2%–51.4%, 15.6%–48.0%, 6.1%–42.8%, and 14.2%–50.9%, respectively. Along with the change of pollution episodes, the variation of local emission contributions for cities within the HCM were not always consistent. For example, largest local contribution to CC, LY, SH, SY were found during WHEP4, while largest local contribution to HRB, JL, MDJ, YB were found in WHEP3. These spatiotemporal variation mainly be attributed to the local emission, regional meteorological and geographical characteristics (Chang et al., 2019; Chen et al., 2018; Dong et al., 2020). Although the variations of local contribution to cities in the HCM were inconsistent, it was obvious that the average local contributions during polluted episodes (WHEP1-WHEP4, 28.5%) were higher than that during WCEP (25.0%). This result suggests that atmosphere polluted level also plays an important role in the proportions of local source and regional transport contributions (Chang et al., 2019). Overall, higher regional contribution to cities in the HCM suggested that it was of great importance to implement regional joint control strategies for improving the HCM region air quality.

3.4.2. Transport contributions from cities within the HCM

Fig. 4 (a) indicated that local emission were the largest contributors among 14 sub-regions within the D02 (15.2%–48.2%) to most cities within the HCM, except for DQ and LY. For DQ and LY, the largest transport contributions were from QQHR and SP with the mean values of 38.5% and 21.3%, respectively, which were 1.2 and 1.7 times higher than that from local emission. Largest transport contributions to LY from its' surrounding cities might be attributed to its small urban areas and larger emissions of major air pollutants from their neighboring cities (Dong et al., 2020). As shown in Fig. 1(b), the administrative division area of LY is small, which results in less local anthropogenic emissions of air pollutants in this city. Small urban area of LY also makes more cities and regions surrounding LY. These above reasons and the downwind geographical location of LY together resulted in largest transport contributions to PM_{2.5} concentration in LY. The total transport contributions from the HCM region (sum of the rest 10 cities in the HCM) to cities in the HCM were ranged from 2.5% to 50.2% (average 41.3%) during the whole studied period. The total transport contribution from the HCM to QQHR was the least with the value of 2.5%, which could be attributed the geographical location of the QQHR and meteorological condition during the studied period. As shown in Fig. S1, QQHR is located in the northwest border area of the HCM, and always be upwind of the studied region. Except QQHR, total contributions from the HCM to other HCM cities during the whole studied period were ranged from 39.2% to 50.2%, which were significantly larger than the local emission contributions.

From the perspective of individual city contribution from the HCM, transport contributions from adjacent cities were larger than that from non-adjacent cities, and transport contributions from upwind cities were larger than that from the downwind cities. Take CC and HRB (the core cities of the HCM) as examples, SY was the largest contributor (12.3%) from HCM to CC during the whole studied period, followed by HRB accounting for 12.2%, which approximately 2–2.5 times larger than that from non-adjacent cities such as DQ (5.9%), QQHR (5.9%), and SH (5.5%). For HRB, the largest contributor from HCM to HRB was SH with the contribution of 22.8%, followed by CC (7.6%), QQHR (6.8%), and DQ (4.9%). CC was also important transport contributors to JL (24.5%),

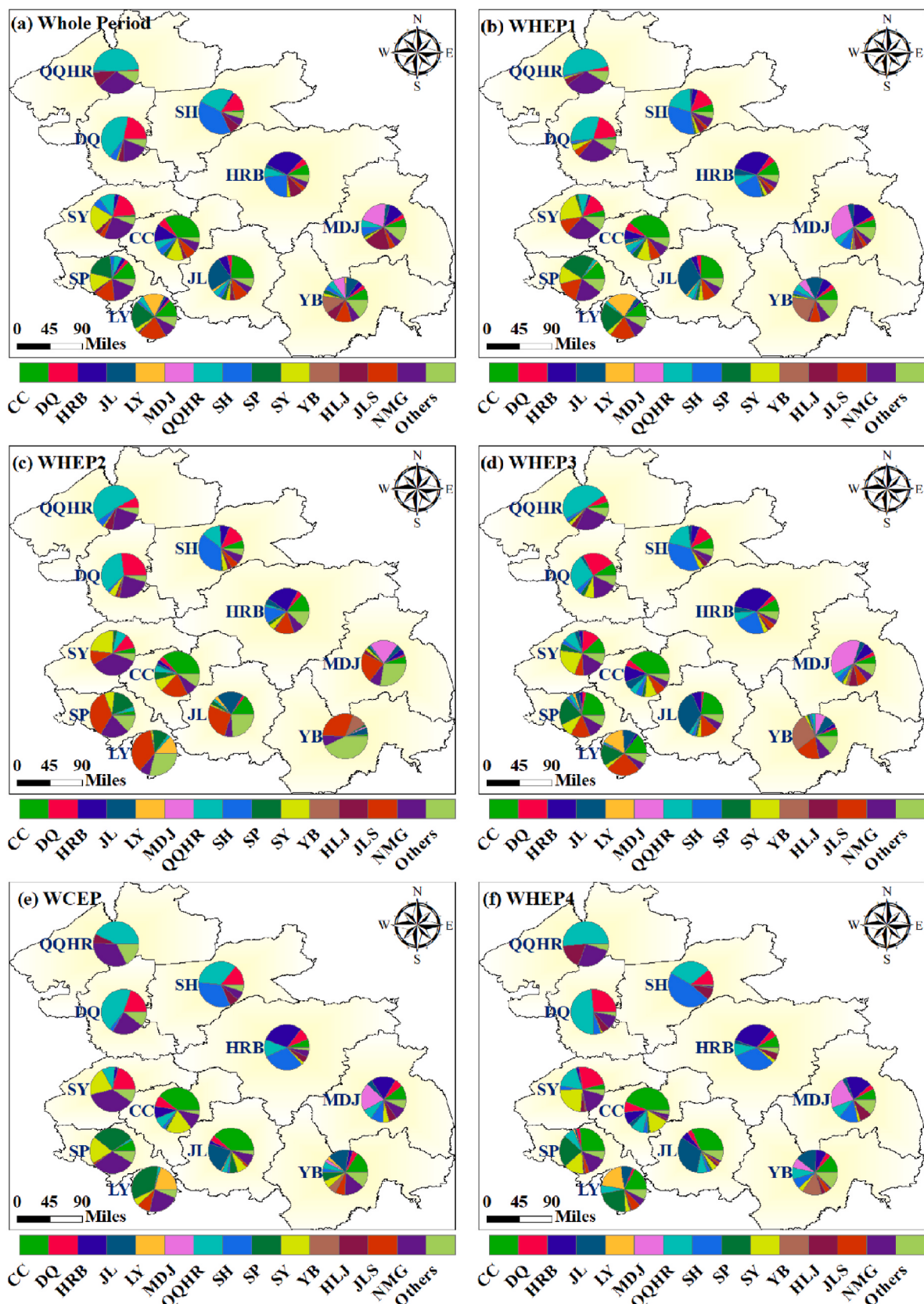


Fig. 4. The temporal variations of inter-cities and regional transport contributions to $\text{PM}_{2.5}$ in the cities within the HCM region.

SP (12.4%), LY (12.3%), YB (8.0%), HRB (7.6%), and MDJ (6.2%). Simultaneously, HRB has significant effects on PM_{2.5} concentrations in cities of CC (12.2%), MDJ (11.5%), and JL (6.7%). As shown in Fig. S1 (f), SY and JL are neighboring cities of CC located in the upwind and downwind of CC. Likewise, SH and MDJ are neighboring cities of HRB located in the upwind and downwind of HRB. These results demonstrated that geographical location and wind direction have significant impacts on the transport contributions. In addition, we note that although CC is not in the upwind of HRB, it is the largest contributor in the HCM to HRB. This result might be attributed the larger emission and higher PM_{2.5} concentration in the CC (Chang et al., 2019). The differences in concentrations of PM_{2.5} and its' precursors (SO₂ and NO_x etc.) will promote the active diffusion of these pollutants from CC to HRB, which increases transport contribution from CC to HRB. The annual emission of PM_{2.5}, SO₂, and NO_x are 74,967, 87,476, and 204,323 tons accounting for 16%, 18%, and 17.5% of total HCM emissions (Li et al., 2017; Zheng et al., 2018). Moreover, the emission from QQHR also can have a significant contribution to long distance cities such as MDJ (5.2%) and YB (4.4%), which indicates a long-distance transportation contribution within the HCM.

3.4.3. Transport contributions from regions outside the HCM

In order to investigate the transport contributions from regions outside the HCM, the region outside the HCM and within the D02 were divided into three regions (Fig. 1(b)): NMG (**sub-region 12**), HLJ (**sub-region 13**) and JLS (**sub-region 14**). As shown in Fig. 4, among these three regions, the largest contributor to the PM_{2.5} concentration in the whole HCM was NMG accounting for 9.1%, followed by JLS (5.1%) and HLJ (3.8%) during the whole studied period. As shown in Fig. 4 (b-f), NMG has significant contributions (more than 5%) to most cities in the HCM, especially during WCEP. The contributions from NMG to cities in the HCM during WCEP were ranged from 5% to 36.2%, which indicated significant contributions to all cities in the HCM. The average contribution from NMG to cities in the HCM during WHEP1-WHEP4 (13.6%) was less than that during WCEP (19.3%). The numbers of city in the HCM significant affected by the transport contribution from NMG were 9, 11, 9, and 5, respectively. Cities influenced by HLJ were mainly gathered in its nearby cities such as MDJ (19.1%), QQHR (10.9%), HRB (9.5%) and SH (7.3%) during the whole studied period. JLS had significant contribution to cities in the south HCM, and largest contributions to cities in the HCM were found during WHEP2, when the contributions from JLS to LY, SP, YB, JL, MDJ, CC, and HRB were 36.9%, 35.1%, 29.4%, 26.1%, 21.3%, 19.4%, and 14.1%, respectively. The transport contribution from NMG and JLS to the HCM during WHEP4 were the least, while that from HLJ was the largest (Fig. 4 (f)).

3.4.4. The impacts polluted level on the transport contributions in the HCM

As discussed above, polluted level also plays an important role on the transport contributions in the HCM besides meteorological condition and geographical characteristics. To further understand the effects of air pollution levels on the regional transport contributions among the studied sub-regions, the studied period was classified into several classes based on the cities' mean PM_{2.5} concentrations. In this study, based on the concentration of PM_{2.5}, five classes were defined, namely, excellent, good, lightly polluted, moderately polluted, and heavily polluted. The upper bounds of these five levels were 35, 75, 115 and 150 µg/m³ for PM_{2.5} concentration. The spatiotemporal variation of average inter-city and regional transport contributions to PM_{2.5} in the HCM cities during different polluted levels are presented in Fig. S4. Fig. S4 suggested that along with the polluted level increasing, long-distance transportation within the studied region decrease significantly, and transportation occurs mostly between adjacent cities. Moreover, local contributions to CC and DQ increased significantly from excellent to heavily polluted days, while local contributions to other cities in the HCM presented significantly decrease from excellent to heavily polluted days. These results demonstrated that regional transport increasing is an important

factor in the formation of heavily polluted days for most cities in the HCM. As the contributor, the transport contribution from CC to SP, LY, and JL increased significantly along with the polluted level increased. In addition, as the largest contributor, the transport contribution from QQHR decreased significantly along with the polluted level increased. These opposite variation between CC and QQHR might be attributed to the regional geographical characteristic, pre-existing pollutant concentration and meteorological conditions (Chang et al., 2019). QQHR remained in the upwind during the studied period, heavily polluted days always accompanied by lower wind speeds, which resulted in less transport contribution from QQHR. CC is in the HCM centre, relatively stable atmosphere during the heavily polluted days and larger emission of air pollutants resulted in a sharp increase of PM_{2.5} mass concentration in CC, which increased the concentration difference between CC and neighboring cities, and then increased active diffusion of atmospheric pollutants from CC to adjacent cities.

Furthermore, it was obvious that contributions from NMG and HLJ decreased significantly along with the increase in polluted level. However, the contribution from the JLS to the whole HCM increased significantly from excellent days (0.1 ± 0.6%) to heavily polluted days (7.0 ± 11.8%). Above results suggested that the emission control in JLS could significantly reduce the PM_{2.5} concentration in the HCM during the heavily polluted days and joint prevention and control of the HCM and JLS should be strengthen for further improving the air quality in the HCM.

3.5. Transport paths during different pollution episodes and different pollution levels

Relatively larger contributions (>5%) between the contributor and receptor cities were selected to identify the transport paths during five different pollution episodes and the results are shown in Fig. 5. Both similarities and differences in patterns in the inter-cities transport contributions were found in different pollution episodes. During the WCEP, there were four main transport paths. As shown in Fig. 5(e), the first path was the pollutants transported from NMG to QQHR, DQ, SY, CC, JL, and finally to YB. The second path was from NMG to QQHR, SH, HRB, and lastly to MDJ. The third one was from NMG to SP, and finally to LY and JL. The last one was from NMG and then through SY, CC, JL, and finally to YB. It was clear that the NMG region played an important role in the regional transport contributions to all cities in the HCM region (4.9%–36.2%), and its contributions can reach MDJ (8.5 ± 6.3%) and YB (14.4 ± 8.9%). These results were mainly attributed to the large northwest wind during the clean days.

Contrastingly, during HEP1, five main transport paths were found, and among them, four paths were similar with clean days. However, it should be noted that the transport distance in the northwest direction was shortened. The other path was found from JLS and then through SY, SP, CC and finally to HRB and SH. In addition, the contributions among neighboring cities increased. Similar transport patterns were found between the WHEP2 and the WHEP1. The transport contribution from the JLS direction significantly increased, while the transport contributions from the NMG direction became weaker. The transport contribution from the JLS direction was due to the prevailing wind direction at the central area of the HCM (Fig. 5(c)). For the WHEP3, there were only two transport paths, which were similar with the first and second transport paths during the WCEP. During this period, NMG was still the main transport source outside the HCM region. The contributions from NMG and JLS to the HCM were weak, and the transport of pollutants mainly occurred on two paths, which were similar with the first and second transport paths of the WCEP as well. Overall, NMG and JLS were the main outside contributions to the HCM. NMG was the dominant outside source to the HCM region during relatively clean days, while JLS was the main contribution to the HCM during most heavy pollution days. Fig. 5 and Fig. S1 demonstrates that the regional transport paths and intensity variation are closely related with the wind direction and speed changes

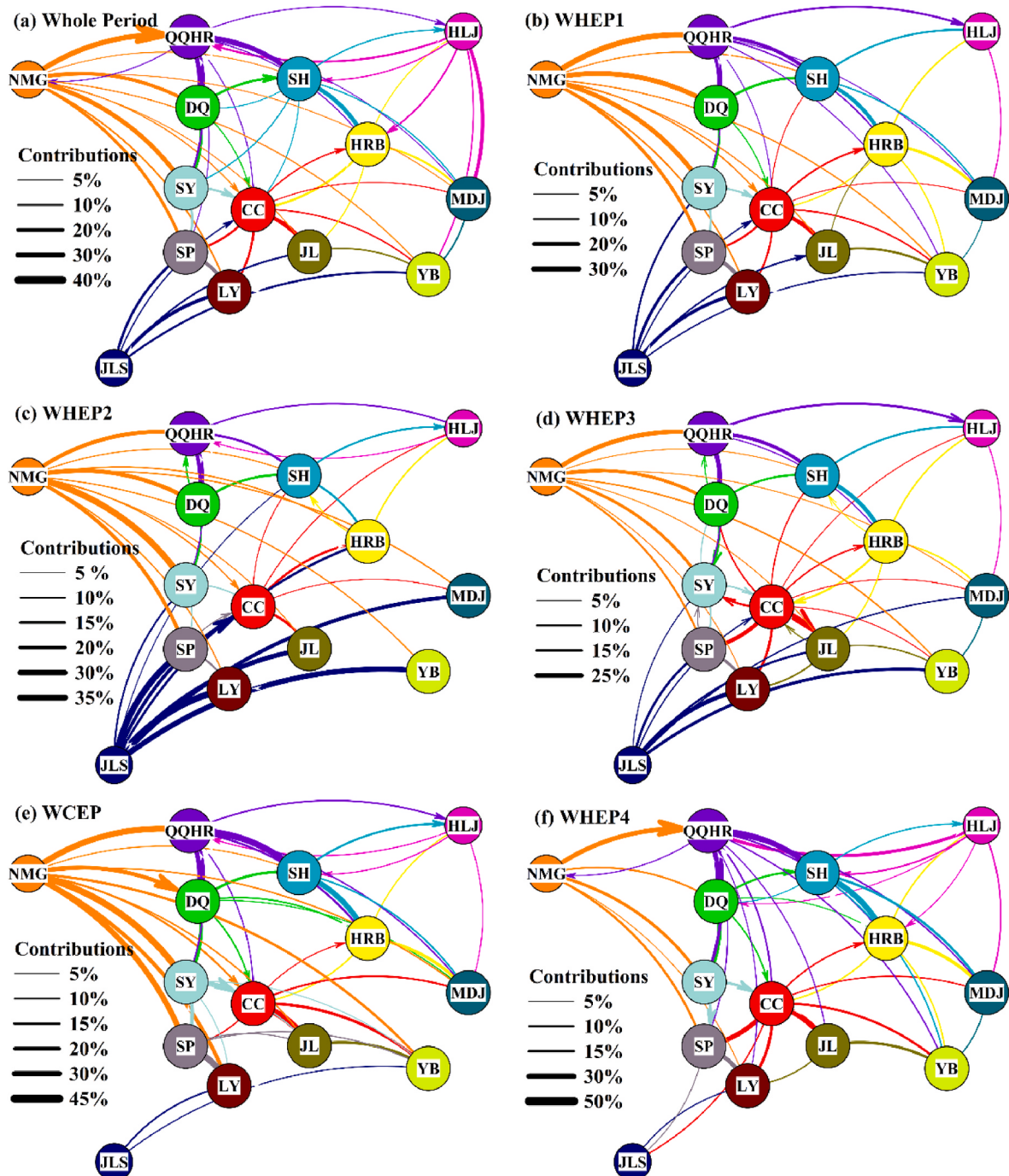


Fig. 5. The main regional transport paths (contributions >5%) of $\text{PM}_{2.5}$ in the D02 region during different episodes (Arrow width and direction represents the magnitude and directions of the transport, respectively).

in studied region, which suggests that we can quantitatively guide the regional joint emergency prevention and control before and during heavily polluted events based on regional weather forecasts in the future.

4. Conclusion and limitation

In this study, the interaction of $\text{PM}_{2.5}$ pollution among cities in winter in the HCM was systematically studied by using CCM and CMAQ-BFM methods. CCM results suggest strong bidirectional causal relationships of $\text{PM}_{2.5}$ pollution among HCM cities, and the causal relationships during polluted episodes were significantly larger than that

during clean period. Moreover, the influence on local $\text{PM}_{2.5}$ pollution from cities in the west were larger than that from cities in the southeast. The regional transport contributions results demonstrated that although local emission were the largest contributors among 14 regions (15.2%–48.2%) for most cities within the HCM, interactions among cities are also strong. Regional transport was largely contributor to $\text{PM}_{2.5}$ in the HCM cities during the whole studied period, which was average 2.5 times larger than that from local emission. Among three regions outside the HCM, the largest contributor to the $\text{PM}_{2.5}$ concentration in the whole HCM was NMG accounting for 9.1%, followed by JLS (5.1%) and HLJ (3.8%). Along with the polluted level increasing, non-adjacent transportation within the studied region decreased significantly, and

transportation occurred mostly between adjacent cities. In addition, regional transport contribution to most the HCM cities increased significantly from excellent to heavily polluted days. The emission control in JLS could significantly reduce the PM_{2.5} concentration in the HCM during the heavily polluted days and joint prevention and control of the HCM and JLS should be strengthened for further improving the air quality in the HCM. The regional transport paths and intensity variation are closely related with the wind direction and speed changes in studied region, which suggests that we can quantitatively guide the regional joint emergency prevention and control before and during heavily polluted events based on regional weather forecasts in the future.

In addition, it should be noted that CMAQ-BFM sensitive analysis is nearly linearly for primary component of PM_{2.5}, but it ignores the nonlinearity formation of secondary PM_{2.5}, such as nitrate and sulfate (Zhou et al., 2017). Thus, estimated regional transport contribution by the BFM existed uncertainty. Moreover, considering the uncertainties of model simulation due to the complex atmospheric environment, the uncertainty of regional meteorological fields, and emission datasets (Chen et al., 2018), the calculated contributions of regional transport in this study should be considered as approximate values. Furthermore, the impact of meteorological condition on the regional transport could be quite complex and should be further studied in the future.

Credit author statement

Bo Li: Conceptualization, Investigation, Methodology, Writing - Original Draft Preparation, Writing- Reviewing and Editing. **Xiao-fei Shi:** Investigation, Methodology, Software. **Jinpan Jiang:** Investigation, Methodology, Software. **Lu Lu :** Investigation, Methodology, Software. **Li-xin Ma:** Investigation, Data curation, Formal analysis. **Wei Zhang:** Conceptualization; Funding acquisition, Project administration; Resources; Supervision. **Kun Wang:** Conceptualization, Supervision. **Hong Qi:** Conceptualization; Funding acquisition, Project administration; Resources; Supervision.

Declaration of competing interest

The authors declare that they have no known competing financial interests or personal relationships that could have appeared to influence the work reported in this paper.

Data availability

Data will be made available on request.

Acknowledgements

This work was supported by National Key R&D Projects of China [grant numbers 2017YFC0212305]; and the Open Project of State Key Laboratory of Urban Water Resource and Environment, Harbin Institute of Technology, China [grant numbers HC202143], and the Heilongjiang Provincial Key Laboratory of Polar Environment and Ecosystem (HPKLEEE), China [grant numbers 2021011].

Appendix A. Supplementary data

Supplementary data to this article can be found online at <https://doi.org/10.1016/j.envres.2023.115360>.

References

- Appel, K.W., Napelenok, S.L., Foley, K.M., Pye, H.O.T., Hogrefe, C., Luecken, D.J., et al., 2017. Description and evaluation of the community multiscale air quality (CMAQ) modeling system version 5.1. *Geosci. Model Dev. (GMD)* 10, 1703–1732.
- Bates, J.T., Weber, R.J., Verma, V., Fang, T., Ivey, C., Liu, C., et al., 2018. Source impact modeling of spatiotemporal trends in PM2.5 oxidative potential across the eastern United States. *Atmos. Environ.* 193, 158–167.
- Boylan, J.W., Russell, A.G., 2006. PM and light extinction model performance metrics, goals, and criteria for three-dimensional air quality models. *Atmos. Environ.* 40, 4946–4959.
- Burr, M.J., Zhang, Y., 2011. Source apportionment of fine particulate matter over the Eastern U.S. Part I: source sensitivity simulations using CMAQ with the Brute Force method. *Atmos. Pollut. Res.* 2, 300–317.
- Chang, X., Wang, S., Zhao, B., Xing, J., Liu, X., Wei, L., et al., 2019. Contributions of inter-city and regional transport to PM2.5 concentrations in the Beijing-Tianjin-Hebei region and its implications on regional joint air pollution control. *Sci. Total Environ.* 660, 1191–1200.
- Chatani, S., Shimadera, H., Itahashi, S., Yamaji, K., 2020. Comprehensive analyses of source sensitivities and apportionments of PM2.5 and ozone over Japan via multiple numerical techniques. *Atmos. Chem. Phys.* 20, 10311–10329.
- Chen, W., Tong, D.Q., Dan, M., Zhang, S., Zhang, X., Pan, Y., 2017. Typical atmospheric haze during crop harvest season in northeastern China: a case in the Changchun region. *J. Environ. Sci. (China)* 54, 101–113.
- Chen, Z., Xie, X., Cai, J., Chen, D., Gao, B., He, B., et al., 2018. Understanding meteorological influences on PM2.5 concentrations across China: a temporal and spatial perspective. *Atmos. Chem. Phys.* 18, 5343–5358.
- Chen, Z., Xu, B., Cai, J., Gao, B., 2016. Understanding temporal patterns and characteristics of air quality in Beijing: a local and regional perspective. *Atmos. Environ.* 127, 303–315.
- Dong, Z., Wang, S., Xing, J., Chang, X., Ding, D., Zheng, H., 2020. Regional Transport in Beijing-Tianjin-Hebei Region and its Changes during 2014–2017: the Impacts of Meteorology and Emission Reduction. *Science of the Total Environment*, p. 737.
- Fu, X., Cheng, Z., Wang, S., Hua, Y., Xing, J., Hao, J., 2016. Local and regional contributions to fine particle pollution in winter of the Yangtze River Delta, China. *Aerosol Air Qual. Res.* 16, 1067–1080.
- Guo, R., Wu, T., Liu, M., Huang, M., Stendardo, L., Zhang, Y., 2019. The construction and optimization of ecological security pattern in the harbin-changchun urban agglomeration, China. *Int. J. Environ. Res. Publ. Health* 16.
- Huang, L., Zhu, Y.H., Zhai, H.H., Xue, S.H., Zhu, T.Y., Shao, Y., et al., 2021. Recommendations on benchmarks for numerical air quality model applications in China - Part 1: PM2.5 and chemical species. *Atmos. Chem. Phys.* 21, 2725–2743.
- Huang, Y., Deng, T., Li, Z., Wang, N., Yin, C., Wang, S., et al., 2018. Numerical simulations for the sources apportionment and control strategies of PM2.5 over Pearl River Delta, China, part I: inventory and PM2.5 sources apportionment. *Sci. Total Environ.* 634, 1631–1644.
- Li, B., Shi, X.F., Liu, Y.P., Lu, L., Wang, G.L., Thapa, S., et al., 2020. Long-term characteristics of criteria air pollutants in megalopolises of Harbin-Changchun megalopolis, Northeast China: spatiotemporal variations, source analysis, and meteorological effects. *Environ. Pollut. (Amsterdam, Neth.)* 267, 115441.
- Li, L., An, J.Y., Zhou, M., Yan, R.S., Huang, C., Lu, Q., et al., 2015. Source apportionment of fine particles and its chemical components over the Yangtze River Delta, China during a heavy haze pollution episode. *Atmos. Environ.* 123, 415–429.
- Li, M., Liu, H., Geng, G., Hong, C., Liu, F., Song, Y., et al., 2017. Anthropogenic emission inventories in China: a review. *Natl. Sci. Rev.* 4, 834–866.
- Li, R., Mei, X., Wei, L., Han, X., Zhang, M., Jing, Y., 2019. Study on the Contribution of Transport to PM2.5 in Typical Regions of China Using the Regional Air Quality Model RAMS-CMAQ. *Atmospheric Environment*, p. 214.
- Li, T.Y., Deng, X.J., Li, Y., Song, Y.S., Li, L.Y., Tan, H.B., et al., 2018. Transport paths and vertical exchange characteristics of haze pollution in Southern China. *Sci. Total Environ.* 625, 1074–1087.
- Ncep, N.C.E.P., 2000. FNL Operational Model Global Tropospheric Analyses, Continuing from July 1999. Research Data Archive at the National Center for Atmospheric Research, Computational and Information Systems Laboratory, Boulder, CO.
- Osada, K., Ohara, T., Uno, I., Kido, M., Iida, H., 2009. Impact of Chinese anthropogenic emissions on submicrometer aerosol concentration at Mt. Tateyama, Japan. *Atmos. Chem. Phys.* 9, 9111–9120.
- Qiao, X., Guo, H., Tang, Y., Wang, P., Deng, W., Zhao, X., et al., 2019a. Local and regional contributions to fine particulate matter in the 18 cities of Sichuan Basin, southwestern China. *Atmos. Chem. Phys.* 19, 5791–5803.
- Qiao, X., Guo, H., Wang, P., Tang, Y., Ying, Q., Zhao, X., et al., 2019b. Fine particulate matter and ozone pollution in the 18 cities of the sichuan basin in southwestern China: model performance and characteristics. *Aerosol Air Qual. Res.* 19, 2308–2319.
- Qu, K., Wang, X., Xiao, T., Shen, J., Lin, T., Chen, D., et al., 2021. Cross-regional Transport of PM2.5 Nitrate in the Pearl River Delta, China: Contributions and Mechanisms. *Science of the Total Environment*, p. 753.
- Sugihara, G., May, R., Ye, H., Hsieh, C-h., Deyle, E., Fogarty, M., et al., 2012. Detecting causality in complex ecosystems. *Science* 338, 496–500.
- Sun, X., Li, D., Li, B., Sun, S., Yabo, S.D., Geng, J., et al., 2020. Exploring the disparity of inhalable bacterial communities and antibiotic resistance genes between hazy days and non-hazy days in a cold megalacity in Northeast China. *J. Hazard Mater.* 398, 122984.
- Wang, L., Wei, Z., Wei, W., Fu, J.S., Meng, C., Ma, S., 2015. Source apportionment of PM2.5 in top polluted cities in Hebei, China using the CMAQ model. *Atmos. Environ.* 122, 723–736.
- Wang, P., Guo, H., Hu, J., Kota, S.H., Ying, Q., Zhang, H., 2019a. Responses of PM2.5 and O₃ concentrations to changes of meteorology and emissions in China. *Sci. Total Environ.* 662, 297–306.
- Wang, Y., Bao, S., Wang, S., Hu, Y., Shi, X., Wang, J., et al., 2017. Local and regional contributions to fine particulate matter in Beijing during heavy haze episodes. *Sci. Total Environ.* 580, 283–296.

- Wang, Y., Li, Y., Qiao, Z., Lu, Y., 2019b. Inter-city air pollutant transport in the Beijing-Tianjin-Hebei urban agglomeration: comparison between the winters of 2012 and 2016. *J. Environ. Manag.* 250, 109520.
- Wu, D., Fung, J.C.H., Yao, T., Lau, A.K.H., 2013. A study of control policy in the Pearl River Delta region by using the particulate matter source apportionment method. *Atmos. Environ.* 76, 147–161.
- Yang, G., Zhao, H., Tong, D.Q., Xiu, A., Zhang, X., Gao, C., 2020a. Impacts of Post-harvest Open Biomass Burning and Burning Ban Policy on Severe Haze in the Northeastern China. *Science of the Total Environment*, p. 716.
- Yang, X., Xiao, H., Wu, Q., Wang, L., Guo, Q., Cheng, H., et al., 2020b. Numerical Study of Air Pollution over a Typical Basin Topography: Source Appointment of Fine Particulate Matter during One Severe Haze in the Megacity Xi'an. *Science of the Total Environment*, p. 708.
- Yarwood, G., 2005. Updates to the Carbon Bond Chemical Mechanism. CB05.
- Zhang, H., Chen, G., Hu, J., Chen, S.H., Wiedinmyer, C., Kleeman, M., et al., 2014. Evaluation of a seven-year air quality simulation using the Weather Research and Forecasting (WRF)/Community Multiscale Air Quality (CMAQ) models in the eastern United States. *Sci. Total Environ.* 473–474, 275–285.
- Zheng, B., Tong, D., Li, M., Liu, F., Hong, C., Geng, G., et al., 2018. Trends in China's anthropogenic emissions since 2010 as the consequence of clean air actions. *Atmos. Chem. Phys.* 18, 14095–14111.
- Zhou, Y., Zhao, Y., Mao, P., Zhang, Q., Zhang, J., Qiu, L., et al., 2017. Development of a high-resolution emission inventory and its evaluation and application through air quality modeling for Jiangsu Province, China. *Atmos. Chem. Phys.* 17, 211–233.